produced striking nuclear fragmentation in essentially all myocytes (Fig. 2, E and F). The fragmentation typically was not random; instead, the nuclear GFP was segregated into two satellite fragments flanking a shrunken or even absent nuclear remnant (Fig. 2F, arrow). In other myocytes, the GFP was diffusely fragmented, with no nucleus apparent by fluorescence or Normarski microscopy (Fig. 2F, arrowhead). The number of GFP-positive muscle nuclei was significantly reduced, which is consistent with cell death (Fig. 2K). *daf-2(e1370)* protected myocytes from both nuclear fragmentation and death (Fig. 2, H and K). In neurons with a cytoplasmic GFP marker, hypoxia induced a dramatic axonal beading morphology (Fig. 2I). Hypoxia also reduced the number of GFP(+) neurons. *e1370* mutants did not show neuronal loss and axonal pathology (Fig. 2, J and K).

Through which cells is *daf-2* regulating hypoxic death? Using cell type-specific promoters, Wolkow *et al.* showed that *daf-2(+)* expression in neurons, but not in muscle or intestine, could rescue the long life-span and dauer formation phenotypes of *daf-2(e1370)* (*19*). We used these strains to determine the cell types involved in *daf-2*-mediated organismal death (*4*). Pan-neuronal expression of *daf-2(+)* in a *daf-2(e1370)* background significantly increased hypoxia-induced death (65.0 ± 5.7 % dead; $P < 0.01$ versus *e1370*; Mann–Whitney nonparametric test) compared with *daf-2(e1370)* alone (4.0 ± 0.6% dead) . However, unlike its other phenotypes, *e1370*'s Hyp phenotype was also rescued by muscle expression of *daf-2(+)* (82.8 ± 7.9% dead; $P < 0.01$ versus *e1370*). Intestinal expression did not increase hypoxic death after the standard 20-hour incubation (10.0 ± 4.3 % dead) but it did after longer incubations (41-hour incubation: 100% dead versus 29.7% of *e1370*; $P < 0.01$). The potent rescue of Hyp by neuronal and muscle *daf-2(+)* expression confirms the assignment of the Hyp phenotype to *daf-2*. Consistent with the direct observation of *daf-2*-dependent neuronal and muscle cell death, these data also suggest that *daf-2(+)* expression induces hypoxic death of muscle and neuronal cell types, whose death, perhaps along with other cell types, then kills the organism. Alternatively, neuronal and muscle expression could induce death of other cell types responsible for organismal death. Indeed, cell nonautonomous effects of *daf-2* have been observed for both aging and dauer formation (*19*, *20*).

How might DAF-2 INR so potently regulate hypoxic death? We initially examined *daf-2* mutants because the INR signaling cascade had been found to regulate apoptosis of vertebrate cells. However, vertebrate INR cascades antagonize apoptosis (*21*); thus, reduction of DAF-2 signaling should, if anything, increase cell death. Hypoxic cell death is not, however, exclusively apoptotic, and after severe insults, it may be almost entirely necrotic (*22*). Given the role of the insulin receptor in regulating glucose utilization, alterations in metabolism by *daf-2*(rf) do provide an appealing mechanism for its hypoxia resistance. *daf-2(e1370)* has been found to have lower O_2 consumption than wild type, perhaps prolonging the time needed for depletion of energy stores and subsequent cell death (*23*). However, these results have been questioned on methodologic grounds and not all findings by van Voorhies are consistent with a metabolic mechanism for *daf-2*'s regulation of hypoxic sensitivity (*24*). Identification of additional Hyp mutants and genes downstream of *daf-16* should clarify the mechanisms underlying *daf-2*'s regulation of hypoxic cell death.

References and Notes

1. M. M. Metzstein, G. M. Stanfield, H. R. Horvitz, *Trends Genet.* **14**, 410 (1998).
2. J. A. Wingrove, P. H. O'Farrell, *Cell* **98**, 105 (1999).
3. A. C. Epstein *et al.*, *Cell* **107**, 43 (2001).
4. Materials and methods are available as supporting material on *Science* Online.
5. K. D. Kimura, H. A. Tissenbaum, Y. Liu, G. Ruvkun, *Science* **277**, 942 (1997).
6. T. Finkel, N. J. Holbrook, *Nature* **408**, 239 (2000).
7. D. Gems *et al.*, *Genetics* **150**, 129 (1998).
8. J. Z. Morris, H. A. Tissenbaum, G. Ruvkun, *Nature* **382**, 536 (1996).
9. S. Paradis, G. Ruvkun, *Genes Dev.* **12**, 2488 (1998).
10. S. Paradis, M. Ailion, A. Toker, J. H. Thomas, G. Ruvkun, *Genes Dev.* **13**, 1438 (1999).
11. S. Ogg, G. Ruvkun, *Mol. Cell* **2**, 887 (1998).
12. E. B. Gil, E. Malone Link, L. X. Liu, C. D. Johnson, J. A. Lees, *Proc. Natl. Acad. Sci. U.S.A.* **96**, 2925 (1999).
13. V. T. Mihaylova, C. Z. Borland, L. Manjarrez, M. J. Stern, H. Sun, *Proc. Natl. Acad. Sci. U.S.A.* **96**, 7427 (1999).
14. J. B. Dorman, B. Albinder, T. Shroyer, C. Kenyon, *Genetics* **141**, 1399 (1995).
15. P. L. Larsen, P. S. Albert, D. L. Riddle, *Genetics* **139**, 1567 (1995).
16. S. Ogg *et al.*, *Nature* **389**, 994 (1997).
17. S. Murakami, T. E. Johnson, *Curr. Biol.* **11**, 1517 (2001).
18. B. A. Scott, M. S. Avidan, C. M. Crowder, unpublished data.
19. C. A. Wolkow, K. D. Kimura, M. S. Lee, G. Ruvkun, *Science* **290**, 147 (2000).
20. J. Apfeld, C. Kenyon, *Cell* **95**, 199 (1998).
21. R. O'Connor, C. Fennelly, D. Krause, *Biochem. Soc. Trans.* **28**, 47 (2000).
22. P. Nicotera, M. Leist, L. Manzo, *Trends Pharmacol. Sci.* **20**, 46 (1999).
23. W. A. Van Voorhies, S. Ward, *Proc. Natl. Acad. Sci. U.S.A.* **96**, 11399 (1999).
24. B. P. Braeckman, K. Houthoofd, A. De Vreese, J. R. Vanfleteren, *Mech. Ageing Dev.* **123**, 105 (2002).
25. A. Fire *et al.*, *Nature* **391**, 806 (1998).
26. O. Hobert, T. D'Alberti, Y. Liu, G. Ruvkun, *J. Neurosci.* **18**, 2084 (1998).
27. We thank G. Ruvkun, D. Riddle, J. Thomas, C. Kenyon, M. Driscoll, S. Clark, and S. Murakami for generously donating strains used in this work. We thank S. Clark and M. Driscoll for providing *pmec-4::GFP* reporter gene. Some strains were provided by the *Caenorhabditis* Genetics Center funded by the National Institutes of Health National Center for Research Resources. We thank M. Nonet for help with microscopy and K. Kornfeld for critique of the manuscript.

Myeloperoxidase, a Leukocyte-Derived Vascular NO Oxidase

Jason P. Eiserich,[1,2,3]*† Stephan Baldus,[2,3]*‡ Marie-Luise Brennan,[6] Wenxin Ma,[4] Chunxiang Zhang,[4] Albert Tousson,[5] Laura Castro,[2,3] Aldons J. Lusis,[6] William M. Nauseef,[7] C. Roger White,[3,4] Bruce A. Freeman[2,3]†

Myeloperoxidase (MPO) is an abundant mammalian phagocyte hemoprotein thought to primarily mediate host defense reactions. Although its microbicidal functions are well established in vitro, humans deficient in MPO are not at unusual risk of infection. MPO was observed herein to modulate the vascular signaling and vasodilatory functions of nitric oxide (NO) during acute inflammation. After leukocyte degranulation, MPO localized in and around vascular endothelial cells in a rodent model of acute endotoxemia and impaired endothelium-dependent relaxant responses, to which MPO-deficient mice were resistant. Altered vascular responsiveness was due to catalytic consumption of NO by substrate radicals generated by MPO. Thus MPO can directly modulate vascular inflammatory responses by regulating NO bioavailability.

Vascular endothelial dysfunction is an established feature of acute inflammation (*1*, *2*) and is typified by compromised function of the endothelium-derived signaling molecule nitric oxide (NO), which serves to stimulate relaxation of vascular smooth muscle cells. Neutrophils contribute to endothelial dysfunction and altered NO signaling during in-

flammation by mechanisms that remain to be fully defined (3–5). Myeloperoxidase (MPO), a highly expressed hemoprotein in neutrophils (~5% of neutrophil protein), is thought to play a primary role in host defense (6). During neutrophil activation, MPO is released into the phagosome and the extracellular space, where it uses hydrogen peroxide (H_2O_2), derived from the neutrophil's respiratory burst oxidase, to catalyze formation of the microbicidal agent hypochlorous acid (HOCl) and other oxidizing species (7). Because MPO and biomarkers of its enzymatic activity are generally increased at inflammatory foci (3–5, 8, 9), this pathway is thought to contribute to oxidant-dependent alterations in vascular function during inflammation. However, whether MPO directly participates as a mediator of vascular dysfunction during inflammation and its mechanism of action remain unknown.
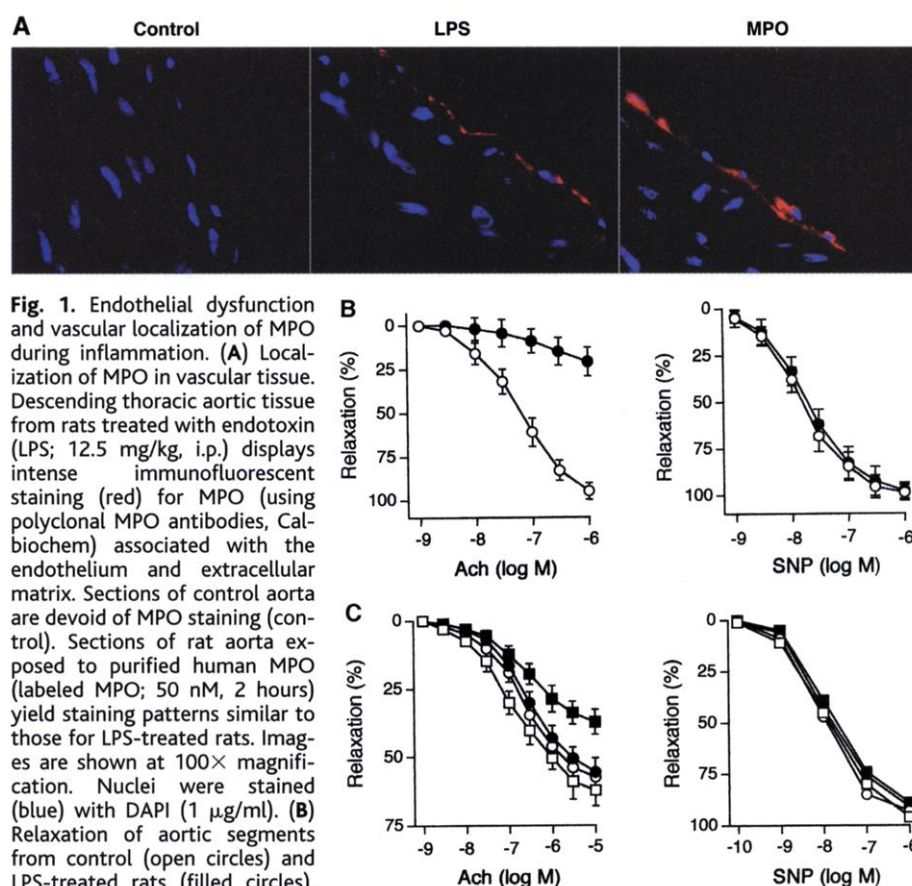
We utilized a rodent model of acute inflammation (endotoxemia) and performed immunohistochemical analysis of vascular MPO distribution. Aortic tissues obtained from rats injected with the Gram-negative bacterial cell-wall component lipopolysaccharide (LPS) revealed endothelial-associated MPO immunoreactivity not present in tissue from control rats (Fig. 1A). MPO was observed on the endothelial surface, within endothelial cells, and in the subendothelial matrix, but not in underlying smooth muscle cells or adherent neutrophils. Because endothelial cells do not express MPO (10), and MPO undergoes apical to basolateral transcytosis across vascular tissues (Fig. 1A, MPO) and cultured endothelial cells (fig. S1) (11, 12), MPO was presumably secreted into the blood vessel lumen by activated leukocytes to then permeate vascular tissue independent of neutrophil extravasation.

Coincident with MPO deposition in vascular tissues (Fig. 1A) (12), ex vivo experiments demonstrated a loss of endothelial function in LPS-treated rats (Fig. 1B), as indicated by reduced responsiveness of precontracted aortic rings to acetylcholine (Ach), which stimulates NO production by endothelial cells. In contrast,

no alterations in the relaxation response were observed in the presence of sodium nitroprusside (SNP), a compound metabolized by vascular smooth muscle cells to locally release NO, indicating that smooth muscle NO-dependent, cyclic guanosine monophosphate (cGMP)–mediated signaling function remained intact. These findings indicate a spatial and temporal association of MPO with altered vascular function during acute inflammation. Similar experiments demonstrated that MPO-deficient mice (13) were resistant to the compromise of Ach-dependent vascular relaxation induced by LPS treatment, as compared to wild-type mice (Fig. 1C). Relaxation induced by SNP remained comparable in all treatment groups. These data reveal that MPO contributes to vascular dysfunction during acute inflammation by modulating endothelial NO production and/or suppressing its bioavailability.

Concentration of MPO in the subendothelial matrix after acute inflammatory responses (Fig. 1A, fig. S1) (12) anatomically poises MPO to modulate endothelial-dependent NO signaling to smooth muscle cells. Treatment of rat aortic segments with purified MPO (50 nM) inhibited

Ach-induced relaxation in an H_2O_2-dependent manner (Fig. 2, A and B), mimicking responses of vessels from LPS-treated rodents. Relaxation of MPO- and H_2O_2-treated vessel segments to SNP was not different from controls (14). Elimination of chloride (Cl⁻) from buffer preparations did not reverse the effect of MPO (Fig. 2B), indicating that diminished vascular relaxation was not attributed to HOCl formation by MPO. Pretreatment of aortic tissues with a low molecular weight heparin (LMWH) decreased binding of MPO (Fig. 2C) and preserved Ach-induced relaxation (Fig. 2B), thus providing a plausible explanation for the anti-inflammatory and vasoprotective properties of heparin analogs (15). Complete relaxation of control rat aortic segments was induced in an agonist-independent manner by the NO donor molecule PAPANO (Fig. 2D). Whereas vessel segments treated with MPO and H_2O_2 achieved complete relaxation comparable to controls, the dose-response curve was right-shifted. These data suggest that compromised vascular relaxation mediated by MPO was due to reduced NO bioavailability and indicated that the mechanism is independent of HOCl production.

[1]Department of Internal Medicine, Division of Nephrology, and Department of Human Physiology, University of California, Davis, CA 95616, USA. [2]Department of Anesthesiology, [3]Center for Free Radical Biology, [4]Department of Medicine, and [5]Imaging Facility, University of Alabama, Birmingham, AL 35233, USA. [6]Department of Microbiology and Molecular Genetics and Department of Medicine, University of California, Los Angeles, CA 90095, USA. [7]Department of Medicine and the Inflammation Program, Veterans Administration Medical Center and University of Iowa, Iowa City, IA 52242, USA.

*These authors contributed equally to this work.
†To whom correspondence should be addressed. E-mail: jpeiserich@ucdavis.edu or bruce.freeman@ccc.uab.edu
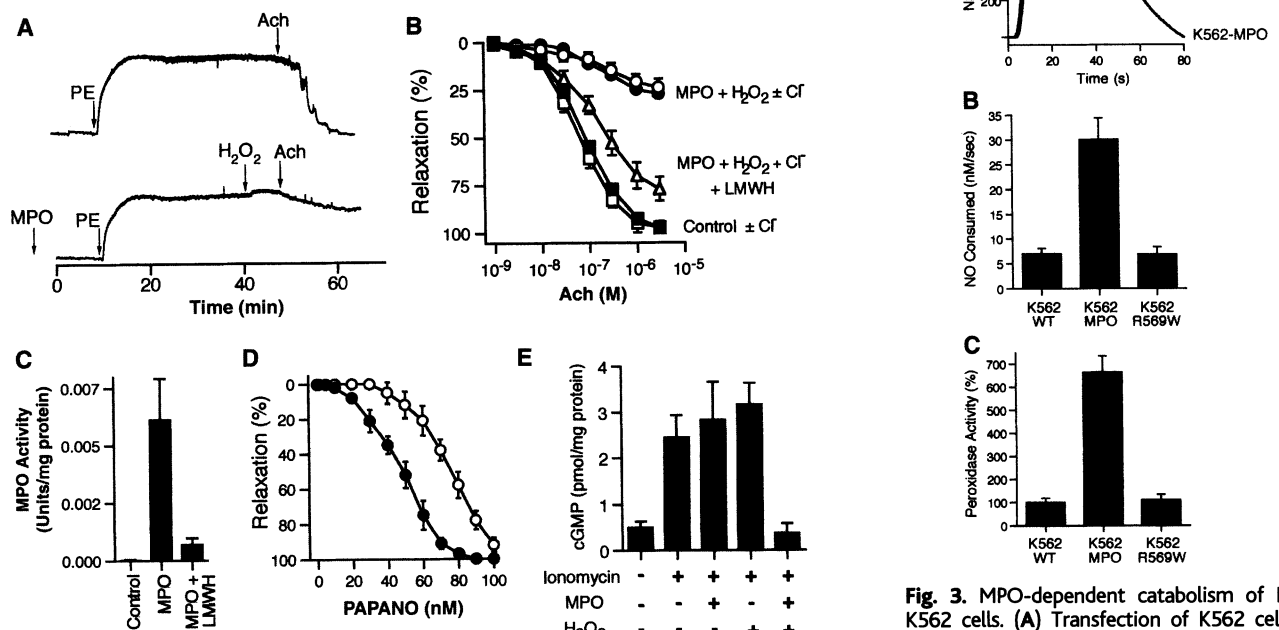‡Present address: Department of Cardiology, University Hospital Eppendorf, Hamburg, Germany.

Fig. 1. Endothelial dysfunction and vascular localization of MPO during inflammation. (A) Localization of MPO in vascular tissue. Descending thoracic aortic tissue from rats treated with endotoxin (LPS; 12.5 mg/kg, i.p.) displays intense immunofluorescent staining (red) for MPO (using polyclonal MPO antibodies, Calbiochem) associated with the endothelium and extracellular matrix. Sections of control aorta are devoid of MPO staining (control). Sections of rat aorta exposed to purified human MPO (labeled MPO; 50 nM, 2 hours) yield staining patterns similar to those for LPS-treated rats. Images are shown at 100× magnification. Nuclei were stained (blue) with DAPI (1 μg/ml). (B) Relaxation of aortic segments from control (open circles) and LPS-treated rats (filled circles). Aortic segments were preconstricted with phenylephrine (PE) and the relaxant responses to Ach and SNP determined. (C) MPO-deficient mice are resistant to LPS-induced alterations in vasomotor function. Ach- and SNP-dependent relaxation of PE preconstricted aortic segments was evaluated in wild-type and MPO-deficient mice after LPS injection (12.5 mg/kg, 4 hours). MPO⁺/⁺ controls (open squares), MPO⁻/⁻ controls (open circles), MPO⁺/⁺ + LPS (filled squares), MPO⁻/⁻+ LPS (filled circles).

The mechanism of MPO-dependent impairment of vascular NO signaling was further explored with a coculture system composed of endothelial cells cultured on a micropore filter placed in close apposition to rat aortic smooth muscle cells (RASMCs). Stimulation of bovine aortic endothelial cell (BAEC) NO synthesis with the calcium ionophore ionomycin (5 μM) induced increased RASMC cGMP production, the product of NO-dependent guanylate cyclase activation and mediator of relaxation (Fig. 2E). Although pretreatment of BAEC monolayers with either MPO or H_2O_2 alone had no effect on ionomycin-induced cGMP production, exposure to MPO and H_2O_2 in concert decreased NO-dependent stimulation of RASMC cGMP synthesis to basal levels. The activity of BAEC NO synthase and smooth muscle cell viability were not altered by this treatment (14). These observations reinforce the notion that MPO, sequestered within vascular tissues after transcytosis or phagocyte extravasation, modulates vasomotor function by altering NO-dependent signaling pathways.
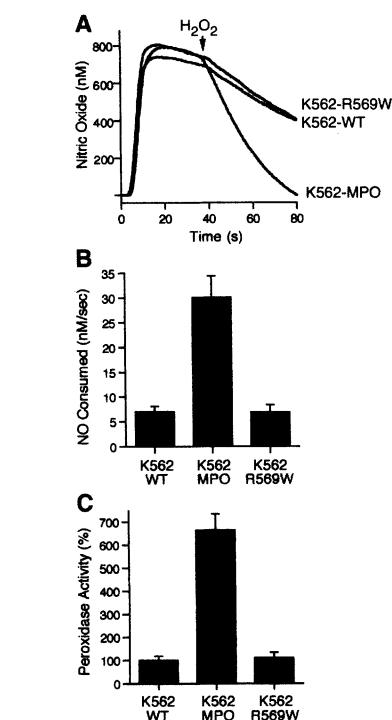
Several lines of evidence suggest that the mechanism underlying MPO-dependent alteration in endothelial-mediated relaxant responses may involve the direct interaction of MPO with NO. The catalytic activity of MPO is biphasically modulated by NO (16, 17); conversely, this implies that the functions of NO could be enzymatically regulated by MPO. Because H_2O_2-activated horseradish peroxidase (HRP) and MPO react rapidly with NO (18, 19), we reasoned that NO catabolism by MPO located within vascular endothelial cells may alter NO signaling and impair vascular relaxation. To test this hypothesis, the rate of NO consumption in a human hematopoietic cell line (K562) expressing either normal or mutant MPO (20) was determined. In contrast to wild-type K562 cells, which do not express MPO, those transfected with normal human MPO (K562-MPO) displayed an increase (~fourfold) in the rate of NO consumption when provided H_2O_2 as substrate (Fig. 3, A and B). This was also consistent with an increase (~sixfold) in

peroxidase activity (Fig. 3C). Transfected cells expressing a catalytically inactive form of MPO harboring a single missense mutation (substitution of tryptophan for arginine 569, K562-R569W) commonly expressed in hereditary human MPO deficiency (21) displayed NO consumption rates (Fig. 3, A and B) and peroxidase activity (Fig. 3C) comparable to wild-type K562 cells. Thus, the membrane-bound and intracellular MPO observed in endothelial cells of vascular tissues during an acute inflammatory response (Fig. 1A), or MPO in leukocytes themselves, can catalytically consume NO.

To determine the mechanism by which MPO consumes NO, experiments were performed with purified human MPO. MPO and H_2O_2 in concert facilitated rapid consumption

Fig. 3. MPO-dependent catabolism of NO by K562 cells. (A) Transfection of K562 cells with normal human MPO, but not a catalytically inactive mutant, increases H_2O_2-dependent NO catabolism. Real-time traces of NO concentration in phosphate-buffered saline were measured by a NO-specific electrode. Wild-type K562 cells (K562-WT), cells transfected with normal MPO (K562-MPO), and cells transfected with mutant MPO (K562-R569W) were suspended at a density of 1 × 10^6 cells/ml and treated with NO (~800 nM) from a saturated solution of NO (1.7 mM). Reactions were initiated by addition of H_2O_2 (50 μM) at the indicated time point. (B) Rates of NO consumption by the various cell types. Values were calculated from the initial rate of NO consumption after subtraction of background NO consumption before H_2O_2 addition and are expressed as nM/s. (C) Peroxidase activity of cell lysates from the various cell types. Data are expressed as a percentage of K562-WT cell peroxidase activity.

Fig. 2. MPO impairs NO-dependent vascular relaxation and guanylate cyclase activation. (A) MPO attenuates Ach-induced relaxation of rat aortic segments in an H_2O_2-dependent manner. Representative traces for relaxation of control (upper) and MPO- and H_2O_2-treated (lower) aortic segments. Aortic segments were pretreated with MPO (50 nM) for 2 hours, washed, and placed in tissue baths. Phenylephrine (PE) and H_2O_2 were added at the indicated times. Increasing doses of Ach were added sequentially after the initial indication but are not shown for clarity. (B) Dose-response curves for Ach-mediated vascular relaxation. Control (squares); MPO (50 nM) + H_2O_2 (10 μM) (circles); LMWH (100 μg/ml) cotreatment with MPO (50 nM) + H_2O_2 (10 μM) (triangles). Experiments were performed in the presence (open symbols) or absence (filled symbols) of chloride. Treatment with MPO or H_2O_2 alone did not affect relaxation (14). (C) LMWH pretreatment inhibits MPO association with aortic tissue. Aortic segments were treated with LMWH (100 μg/ml) for 1 hour, then incubated with MPO (50 nM) for 2 hours, and tissue-associated peroxidase activity was determined. (D) MPO inhibits relaxation of aortic segments induced by the NO donor PAPANO. Control (filled circles); MPO (50 nM) pretreatment + H_2O_2 (10 μM) (open circles). Treatment with H_2O_2 was performed after aortic segments were preconstricted with phenylephrine, and immediately before addition of Ach or PAPANO. (E) RASMC production of cGMP when cocultured with BAECs on adjacent Transwell plate micropore filters. BAECs were stimulated with ionomycin (5 μM) to produce NO and, in some cases, were preincubated with MPO (13 nM) and/or H_2O_2 (10 μM) before ionomycin stimulation.

of NO (Fig. 4A) consistent with previous observations (18, 19). Despite the nearly 300-fold greater concentration of NO relative to MPO, complete consumption of NO indicated a catalytic mechanism. The reaction of NO with compounds I and II of the prototypical heme peroxidase HRP is rapid; the second-order rate constants are 7.0×10^5 and $1.3 \times 10^6 \text{ M}^{-1}\text{s}^{-1}$, respectively (18). Despite unequivocal evidence demonstrating catalytic consumption of NO by heme peroxidases, the physiological relevance of this reaction pathway can be challenged on kinetic terms; stated another way, physiologic levels of NO (10 nM to 1 μM) are unlikely to compete with much more abundant substrates of MPO (i.e., ascorbate and tyrosine) given the similar rates of reaction [$k \sim 10^6$ $\text{M}^{-1}\text{s}^{-1}$ (18, 22–24)]. To address this issue, experiments were performed in human blood plasma, a representative extracellular fluid containing most, if not all, possible competitive physiological substrates of MPO. Steady-state concentrations of ~0.8 μM NO in plasma were achieved by PAPANO (25 μM), with MPO addition facilitating rapid consumption of NO in an H_2O_2-dependent manner (Fig. 4B). Whereas low molecular weight reductants in extracellular fluids would be expected to competitively inhibit the reaction of NO with MPO, physiologic levels of both tyrosine and ascorbate accelerated MPO-dependent consumption of NO (Fig. 4C). Trolox, a phenolic water-soluble analog of α-tocopherol and known substrate of MPO (22), completely inhibited NO consumption. As ascorbate, tyrosine, and Trolox undergo one-electron oxidation by MPO (22–24), forming their respective radicals, the previous observation that NO is consumed at rates near the diffusion limit (2×10^9 $\text{M}^{-1}\text{s}^{-1}$) by reaction with the tyrosyl radical (25), but not the Trolox radical (26), lends insight into these observations. Like tyrosyl radicals, ascorbyl radicals generated by ascorbate oxidase appear to consume NO in both blood plasma and phosphate-buffered solutions (Fig. 4D). Consumption of NO in blood plasma was sustained until ascorbate levels were depleted, at which time NO returned to steady-state levels. Restoring ascorbate to the reactions reinitiated NO catabolism. These data reveal that under physiological conditions, NO consumption by MPO occurs by reaction with substrate radicals generated by MPO (Fig. 4E), in preference to the active-site heme, and is a pathway operative in complex biological fluids.

In addition to catalyzing microbicidal functions, our observations reveal that MPO modulates NO-dependent signaling processes during inflammation. Whereas this function was exemplified in the context of the mammalian vasculature, the data reveal additional mechanisms for modulating the actions of NO in diverse physiologic and pathologic contexts. For NO to serve as a versatile signaling molecule, its bioavailability must be under exquisite control. The data presented herein show that heme peroxidases can provide such a regulatory function, and that this may be common to many organisms given the highly conserved structure and catalytic activity of heme peroxidases across diverse phylogeny. A reappraisal of heme peroxidase function involving NO may expose previously unrecognized phenotypic consequences of MPO deficiency in humans (27).

References and Notes

1. A. B. Lentsch, P. A. Ward, J. Pathol. 190, 343 (2000).
2. P. T. Murray, M. E. Wylam, J. G. Umans, Anesth. Analg. 90, 89 (2000).
3. B. C. Sheridan et al., Am. J. Physiol. 271, L820 (1996).
4. N. Sekido et al., Nature 365, 654 (1993).
5. D. J. Lefer, D. M. Flynn, D. C. Anderson, A. J. Buda, Am. J. Physiol. 271, H2421 (1996).
6. S. J. Klebanoff, in Peroxidases in Chemistry and Biology, vol. 1, J. Everse, K. Everse, M. B. Grisham, Eds. (CRC Press, Boca Raton, FL, 1991), pp. 1–35.
7. C. C. Winterbourn, M. C. Vissers, A. J. Kettle, Curr. Opin. Hematol. 7, 53 (2000).
8. G. Deby-Dupont, C. Deby, M. Lamy, Intensivmed. Notfallmed. 36, 500 (1999).
9. J. W. Heinecke, J. Lab. Clin. Med. 133, 321 (1999).
10. W. F. Pendergraft et al., Kidney Int. 57, 1981 (2000).
11. Supplementary figure and details of experimental procedures are available on Science Online.
12. S. Baldus et al., J. Clin. Invest. 108, 1759 (2001).
13. M.-L. Brennan et al., J. Clin. Invest. 107, 419 (2001).
14. J. P. Eiserich et al., unpublished data.
15. D. J. Tyrell, A. P. Horne, K. R. Holme, J. M. Preuss, C. P. Page, Adv. Pharmacol. 46, 151 (1999).
16. J. P. Eiserich et al., Nature 391, 393 (1998).
17. H. M. Abu-Soud, S. L. Hazen, J. Biol. Chem. 275, 5425 (2000).
18. R. E. Glover, V. Koshkin, H. B. Dunford, R. P. Mason, Nitric Oxide 3, 439 (1999).
19. H. M. Abu-Soud, S. L. Hazen, J. Biol. Chem. 275, 37524 (2000).
20. W. M. Nauseef, M. Cogley, S. McCormick, Biol. Chem. 271, 9546 (1996).
21. W. M. Nauseef, S. Brigham, M. Cogley, J. Biol. Chem. 269, 1212 (1994).
22. W. Sun, H. B. Dunford, Biochem. Biophys. Res. Commun. 194, 306 (1993).
23. L. A. Marquez, H. B. Dunford, J. Biol. Chem. 270, 30434 (1995).
24. Y. Hsuanyu, H. B. Dunford, Arch. Biochem. Biophys. 368, 413 (1999).
25. J. P. Eiserich, J. Butler, A. van der Vliet, C. E. Cross, B. Halliwell, Biochem. J. 310, 745 (1995).
26. H. Rubbo, et al., J. Biol. Chem. 275, 10812 (2000).
27. F. Lanza, J. Mol. Med. 76, 676 (1998).
28. We thank J. S. Beckman, C. E. Cross, A. van der Vliet, and A. M. Corbacho for insightful discussions and M. Goedken, P. H. Chumley, T. V. Bamberg, and J. Hurt for technical assistance. This work was supported by grants from the National Institutes of Health (B.A.F., C.R.W., W.M.N., and A.J.L.), the American Heart Association (J.P.E.), the Paul F. Gulyassy Endowed Professorship (J.P.E.), and the Department of Veterans Affairs, (W.M.N.). Support for S.B. was provided by the Deutsche Herzstiftung and the Max Planck Gesellschaft.

Fig. 4. Catalytic consumption of NO by MPO. (**A**) Real-time measurements of NO consumption were performed using a NO-specific electrode. Adding NO (1.7 μM) to buffer 50 mM NaH_2PO_4, 140 mM NaCl, pH 7.4) resulted in a rapid peak that slowly decayed. Providing MPO (13 nM) or H_2O_2 (5 μM) alone had no effect on the rate of decay. Combined treatment with MPO and H_2O_2 induced rapid loss of NO (upper and lower traces are reverse order of addition). (**B**) MPO-dependent consumption of NO in human blood plasma is dependent on H_2O_2. About 4 to 6 min after PAPANO (25 μM) addition to blood plasma, NO reached a steady-state concentration of ~0.8 μM. MPO (26 nM) and H_2O_2 (10 μM) were added at the times indicated. The trace is representative of four separate experiments using plasma from different donors. (**C**) Physiological levels of tyrosine (Tyr) or ascorbate (Asc) accelerate MPO-dependent consumption of NO, whereas Trolox inhibits NO consumption; MPO (0.8 nM) and NO (~800 nM, added as a bolus). (**D**) Ascorbyl radicals consume NO in blood plasma (upper trace) and buffer solutions (lower trace). NO was generated in plasma by adding PAPANO (25 μM), and ascorbyl radicals were generated by addition of ascorbate oxidase (AO, 0.5 U/ml). Consumption of NO in plasma was rapid and continued until Asc levels were depleted, at which time NO returned to steady-state levels; restoring Asc (100 μM) to plasma reinitiated NO consumption. In buffer solutions, NO (1.7 μM) was added as a bolus, and AO (0.5 U/ml) and Asc (150 μM) were provided as indicated. Data are representative of four separate experiments. (**E**) Proposed physiological mechanism for MPO-dependent NO catabolism to nitrite (NO_2^-) by radical products of MPO catalysis. MPO-I, MPO compound I; MPO-II, MPO compound II; RH, reducing substrate; R˙, one-electron oxidized radical product of RH.